

Collective Cell Movement Promotes Synchronization of Coupled Genetic Oscillators

Koichiro Uriu,* and Luis G. Morelli†

*Theoretical Biology Laboratory, RIKEN, 2-1 Hirosawa, Wako, Saitama 351-0198, Japan;

†Departamento de Física, FCEyN UBA and IFIBA, CONICET; Pabellón 1, Ciudad Universitaria, 1428 Buenos Aires, Argentina

SUPPLEMENTARY MATERIAL

Movie S1 Phase profiles for $v_0/\mu = 0.03$ and $\kappa_\varphi/D_\varphi = 0$ in Eqs. 1-5 in the main text. The color indicates the intensity determined by $(1 + \sin \theta_i)/2$ as in Fig. 2. For clear visualization, we ran a simulation in a domain 12×12 . Other parameters are $N = 200$, $v_0 = 1.2$, $D_\varphi = 0.5$, $\omega = 2.1$, and $D_\theta = 0.1$.

Movie S2 Phase profiles for $v_0/\mu = 0.12$ and $\kappa_\varphi/D_\varphi = 0$ in Eqs. 1-5 in the main text. The domain size and other parameters are the same as in Movie S1.

Movie S3 Phase profiles for $v_0/\mu = 1.2$ and $\kappa_\varphi/D_\varphi = 0$ in Eqs. 1-5 in the main text. The domain size and other parameters are the same as in Movie S1.

Movie S4 Phase profiles for $v_0/\mu = 0.12$ and $\kappa_\varphi/D_\varphi = 3.2$ in Eqs. 1-5 in the main text. The domain size and other parameters are the same as in Movie S1.

Movie S5 Phase profiles for $v_0/\mu = 0.12$ and $\kappa_\varphi/D_\varphi = 1.6$ in Eqs. 1-5 in the main text. The domain size and other parameters are the same as in Movie S1.

Movie S6 Stable kinematic phase wave for $v_0/\mu = 0.12$ and $\kappa_\varphi/D_\varphi = 0$ in Eqs. 1-5 in the main text. Other parameters are $L = 24$, $N = 800$, $v_0 = 1.2$, $D_\varphi = 0.5$, $\omega = 2.1$, and $D_\theta = 0.1$.

Movie S7 Unstable kinematic phase wave for $v_0/\mu = 0.12$ and $\kappa_\varphi/D_\varphi = 1.6$ in Eqs. 1-5 in the main text. Other parameters are the same as in Movie S6.

Movie S8 Stable kinematic phase wave for $v_0/\mu = 1.2$ and $\kappa_\varphi/D_\varphi = 1.6$ in Eqs. 1-5 in the main text. $\mu = 1$. Other parameters are the same as in Movie S6.

Text S1 (including Figures S1 and S2) Analyses on a disk model and a Voronoi model including adhesive forces between cells.

Collective Cell Movement Promotes Synchronization of Coupled Genetic Oscillators

Koichiro Uriu,* and Luis G. Morelli†

*Theoretical Biology Laboratory, RIKEN, 2-1 Hirosawa, Wako, Saitama 351-0198, Japan;

†Departamento de Física, FCEyN UBA and IFIBA, CONICET; Pabellón 1, Ciudad Universitaria, 1428 Buenos Aires, Argentina

Text S1

Disk model

In the main text, we describe a tissue by a Voronoi diagram, Fig. 1A. Here we consider an alternative description in which we represent cells as disks of diameter one in a two-dimensional space, Fig. S1A, to confirm that our results hold in different descriptions of the tissue.

In this disk model, the over-damped equation for the position \mathbf{x}_i of cell i reads

$$\frac{d\mathbf{x}_i(t)}{dt} = v_0 \mathbf{n}_i(t) + \mu \sum_{\substack{j=1 \\ j \neq i}}^N \mathbf{F}(\mathbf{x}_i, \mathbf{x}_j), \quad (\text{S1})$$

with repulsive intercellular forces Eq. 2 in the main text. The time evolution of the angle $\varphi_i(t)$ for the polarity of self-propelled motion $\mathbf{n}_i(t)$ is given by Eq. 3 in the main text.

While the Voronoi diagram determines the neighbors of cells and their contact lengths, in the disk model we have to specify them. We introduce the coupling range r_θ for the equation of coupled phase oscillators in the disk model. When the distance r_{ij} between cells i and j is shorter than r_θ , they can interact with each other. The time evolution of the phase of oscillation θ_i for cell i reads

$$\frac{d\theta_i(t)}{dt} = \omega + \frac{1}{n_i(t)} \sum_{r_{ij} \leq r_\theta} \sin[\theta_j(t) - \theta_i(t)] + \sqrt{2D_\theta} \xi_i(t), \quad (\text{S2})$$

where $n_i(t)$ is the number of cells within the coupling range r_θ of cell i , at time t .

To generate gap spaces between cells, we choose a lower cell density in the disk model than in the Voronoi model in the main text, Fig. S1A. As the ratio of polarity alignment strength to polarity noise κ_φ/D_φ grows, the velocity order parameter $\langle \Phi \rangle$ displays a transition from very low values to high values, indicating that cells develop correlated movement for large alignment strength, Fig. S1B. Due to the sparse density, the velocity order parameter does not reach 1 but saturates at around 0.7 even with a large κ_φ/D_φ . Cell movement with short-range velocity correlations enhances synchronization more than movement without correlation, Fig. S1C and D, confirming that our results do not depend on the particular choice of tissue description and density. This efficient synchronization for intermediate alignment strengths correlates with a larger mixing rate, see Fig. S1E.

Cell adhesion

In the main text, we consider only a repulsive force between cells for simplicity. Here we confirm that results in the main text are qualitatively the same when we allow for the presence of an adhesive force between cells.

We describe a tissue by a Voronoi diagram and include an adhesive force between cells in the over-damped equation:

$$\frac{d\mathbf{x}_i(t)}{dt} = v_0 \mathbf{n}_i(t) + \mu \sum_{j \in V_i(t)} \mathbf{F}(\mathbf{x}_i, \mathbf{x}_j) + \mu_a \sum_{j \in V_i(t)} \mathbf{F}_a(\mathbf{x}_i, \mathbf{x}_j), \quad (\text{S3})$$

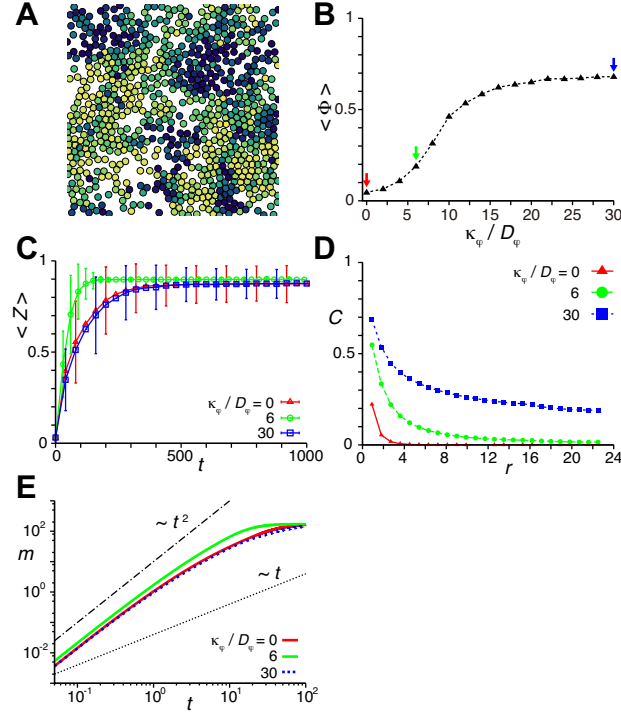


Figure S1: A short-range velocity correlation enhances synchronization in a disk model. (A) Disks with diameter one represent cells. (B) Velocity order parameter $\langle \Phi \rangle$ as a function of the ratio of the polarity alignment strength to the polarity noise intensity, κ_ψ / D_ψ . Arrows point to $\kappa_\psi / D_\psi = 0$ (red), 6 (green), and 30 (blue). (C) Time evolution of average phase order parameter $\langle Z(t) \rangle$ for different ratios κ_ψ / D_ψ as indicated, in the disk model Eqs. S1 and S2. Error bars indicate the SD. (D) Velocity cross-correlation C as a function of the distance r for different ratios κ_ψ / D_ψ as indicated. (E) Time evolution of $m(t)$ for the same values of κ_ψ / D_ψ as in (C). In all panels, $L = 32$, $N = 800$, $v_0 = 1.2$, $\mu = 10$, $D_\psi = 0.5$, $\omega = 2.1$, $r_\theta = 1.2$ and $D_\theta = 0.1$ in Eqs. 2, 3, S1 and S2.

where $\mathbf{F}(\mathbf{x}_i, \mathbf{x}_j)$ is the repulsive force described by Eq. 2 in the main text, μ_a is the coefficient of adhesive force strength and $\mathbf{F}_a(\mathbf{x}_i, \mathbf{x}_j) = F_a(\mathbf{x}_i, \mathbf{x}_j)\mathbf{e}_{ij}$ is the adhesive force with $\mathbf{e}_{ij} = (\mathbf{x}_j - \mathbf{x}_i)/|\mathbf{x}_j - \mathbf{x}_i|$,

$$F_a(\mathbf{x}_i, \mathbf{x}_j) = \begin{cases} 0, & r_{ij} \leq 1 \\ l_{ij}(r_{ij} - 1), & r_{ij} > 1 \end{cases} \quad (\text{S4})$$

and $r_{ij} = |\mathbf{x}_j - \mathbf{x}_i|$. l_{ij} is the contact length between cells i and j . We assume that the adhesive force between cells i and j is caused by adhesion molecules distributed uniformly on cell surfaces. Under this assumption, if the contact length between two cells is longer, the adhesive force \mathbf{F}_a becomes stronger. We also assume that the adhesive force \mathbf{F}_a depends linearly on the distance between two cells. Because the contact length between two cells tends to decrease as their distance increases, F_a is a non-monotonic function of r_{ij} , Fig. S2A.

We generate collective cell movement with Eqs. 3, S3 and S4. A stronger adhesive force makes cells less mobile, Fig. S2B. We find that the adhesive force facilitates collective cell movement: cells attain a larger value of velocity order parameter with a lower value of κ_ψ / D_ψ , Fig. S2C. We confirm that the correlation of cell movement with a lengthscale of $2 \sim 3$ cell diameters is optimal for the synchronization of coupled phase oscillators even in the presence of cell adhesion, see $\kappa_\psi / D_\psi = 1$ in Fig. S2D.

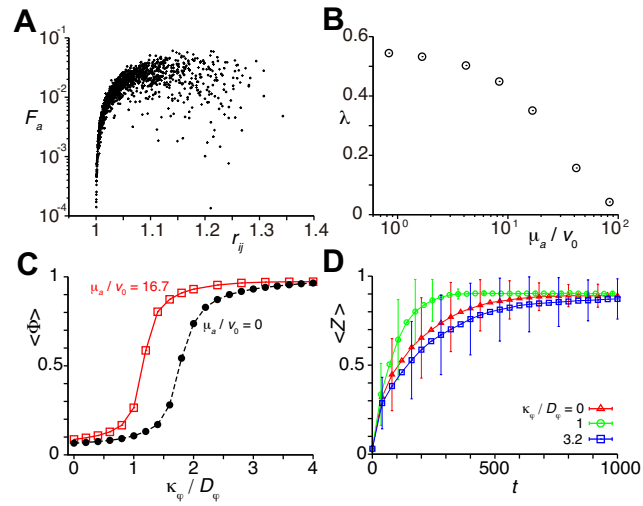


Figure S2: A short-range velocity correlation enhances synchronization in the presence of an adhesive force between cells. (A) Dependence of adhesive force F_a defined by Eq. S4 on the intercellular distance r_{ij} in simulations. (B) Dependence of the cell mixing rate λ on the ratio of the coefficient of adhesive force strength μ_a to self-propulsion speed v_0 . (C) Dependence of the average velocity order parameter $\langle \Phi \rangle$ on the ratio of the polarity alignment strength κ_φ to the polarity noise intensity D_φ , in the presence of cell adhesion (red open squares). (D) Time evolution of the average phase order parameter $\langle Z(t) \rangle$ for different ratios κ_φ/D_φ . Error bars indicate the SD. In all panels, $L = 24$, $N = 800$, $v_0 = 1.2$, $\mu = 10$, $D_\varphi = 0.5$, $\omega = 2.1$, and $D_\theta = 0.1$ in Eqs. 2-5, S3 and S4. In (B) $\kappa_\varphi = 0$. In (C) and (D) $\mu_a = 20$.